OVERVIEW OF THE CUMULUS HUMILIS AEROSOL PROCESSING STUDY

BY LARRY K. BERG, CARL M. BERKOWITZ, JOHN A. OGREN, CHRIS A. HOSTETLER, RICHARD A. FERRARE, MANVENDRA K. DUBEY, ELISABETH ANDREWS, RICHARD L. COULTER, JOHNATHAN W. HAIR, JOHN M. HUBBE, YIN-NAN LEE, CLAUDIO MAZZOLENI*, JASON OLFERT+, AND STEPHEN R. SPRINGSTON

During the summer of 2007, CHAPS investigated changes in the chemical and optical properties of aerosols due to their interaction with shallow cumuli.

Aerosols influence climate directly by scattering and absorbing radiation and indirectly through their influence on cloud microphysical and dynamical properties. The Intergovernmental Panel on Climate Change (IPCC) concluded that the global radiative forcing due to aerosols is large and in general cools the planet (Forster et al. 2007). But the uncertainties in these estimates are also large due to our poor understanding of many of the important processes related to aerosols and clouds. To address this uncertainty, Ghan and Schwartz (2007) proposed an integrated strategy for addressing issues related to aerosols and aerosol processes. Using this conceptual framework, the Cumulus Humilis Aerosol Processing Study (CHAPS) is a stage 1 activity, that is, a detailed process study. The specific focus of CHAPS was to provide concurrent observations of the chemical composition of the activated [particles that are currently serving as cloud condensation nuclei (CCN)] and nonactivated aerosols, the scattering and extinction profiles, and detailed aerosol and droplet size spectra in the vicinity of Oklahoma City, Oklahoma, during June 2007.

Numerous campaigns have examined aerosol properties downwind from large pollution sources, including the Megacity Initiative: Local and Global

AFFILIATIONS: BERG, BERKOWITZ, AND HUBBE—Pacific Northwest National Laboratory, Richland, Washington; OGREN—NOAA Earth System Research Laboratory, Boulder, Colorado; HOSTETLER, FERRARE, AND HAIR—NASA Langley Research Center, Hampton, Virginia; DUBEY AND MAZZOLENI—Los Alamos National Laboratory, Los Alamos, New Mexico; ANDREWS—NOAA Earth System Research Laboratory, and Cooperative Institute for Research in Environmental Sciences, University of Colorado, Boulder, Colorado; COULTER—Argonne National Laboratory, Argonne, Illinois; LEE, OLFERT, AND SPRINGSTON—Brookhaven National Laboratory, Upton, New York.
* **CURRENT AFFILIATION:** Michigan Technological University, Houghton, Michigan
+ **CURRENT AFFILIATION:** The University of Alberta, Edmonton, Alberta, Canada
CORRESPONDING AUTHOR: Dr. Larry K. Berg, P.O. Box 999, MSIN K9-30, Richland, WA 99352
E-mail: larry.berg@pnl.gov

The abstract for this article can be found in this issue, following the table of contents.
DOI:10.1175/2009BAMS2760.1

In final form 30 June 2009

Research Observations (MILAGRO) campaign (Molina et al. 2008) and the two of the three Aerosol Characterization Experiments, ACE-2 and ACE-Asia, which are described by Raes et al. (2000) and Huebert et al. (2003), respectively. Other studies conducted near cities have examined changes in both aerosols and clouds downwind of urban areas. For example, Alkezweeny et al. (1993) found that wintertime stratiform clouds associated with the urban plumes of Denver, Colorado, and Kansas City, Missouri, have a larger number concentration and smaller median volume diameter of droplets than clouds that had not been affected by the urban plume. Likewise, Jirak and Cotton (2006) found a decrease in precipitation in polluted regions along the Front Range of the Rocky Mountains. In a modeling study, Van Den Heever and Cotton (2007) found that precipitation downwind of urban areas may be influenced by changes in aerosols as well as the convergence pattern caused by the city. Recently, the New England Air Quality Study (NEAQS), and the 2004 International Consortium for Atmospheric Research on Transport and Transformation (ICARTT; Fehsenfeld et al. 2006), which were conducted during the summer of 2004, examined the transport of pollutants and aerosols eastward from New England over the Atlantic Ocean. The Texas Air Quality Study/Gulf of Mexico Atmospheric Composition and Climate Study (TexAQS/GoMACCS) also looked at relationships between clouds and aerosols in polluted conditions around Houston, Texas (e.g., Sorooshian et al. 2007; Lu et al. 2008). In contrast to these recent studies near large or very dirty cities, CHAPS was conducted near a moderately sized city that is representative of a large number of cities around the United States.

CHAPS was also one of the first times that a Aerodyne aerosol mass spectrometer (AMS; Jayne et al. 2000) was used in conjunction with a counterflow virtual impactor (CVI) inlet (Noone et al. 1993) on an aircraft. The AMS provides information on the nonrefractory (i.e., materials that are chemically and physically unstable at high temperatures) composition of aerosols, while the CVI uses a counterflow relative to the main incoming airstream to exclude small droplets and nonactivated particles from the inlet, allowing only larger cloud droplets to enter the inlet. The combination of the CVI and AMS allow the examination of the chemical composition of the dried aerosol kernel from the cloud droplets.

EXPERIMENTAL GOALS. A key objective of the U.S. Department of Energy's (DOE)'s Atmospheric Sciences Program (ASP; more information is available online at www.asp.bnl.gov) is to improve the understanding of aerosol radiative effects on climate. This objective encompasses not only clear sky observations but also studies relating the effects of both aerosols on clouds and clouds on aerosols—in particular, how clouds affect the chemical and optical properties of aerosols. The latter was the science driver in the design of CHAPS.

The measurement strategy for CHAPS was intended to provide measurements relevant to four questions associated with the aerosol radiative forcing issues of interest to the ASP:

1) How do the below-cloud and above-cloud aerosol optical and cloud nucleating properties downwind of a typical North American city differ from the optical and nucleating properties of aerosols in air unperturbed by urban emissions? Our interest is in the differences in the radiative properties, chemical composition, hygroscopic properties, and size distributions below and above cloud, and upwind and downwind of such a city.
2) How does the distribution of aerosol extinction vary in relation to the proximity to individual clouds and fields of clouds and why?
3) What are the differences, in terms of both size distributions and chemical composition, between activated aerosols within the urban plume and those outside the urban plume? This question is also intended to encompass issues related to differences between particles that have not been activated inside and outside of the urban plume.
4) To what extent can models with state-of-the-art cloud parameterizations capture the statistical features of the below-above-cloud aerosols?

The material in this article presents results from CHAPS illustrating the observations and discussing their relevance to questions 1 and 3 listed above. CHAPS provides a rich set of observations that is publically available at the ASP data archive (available online at ftp://ftp.asd.bnl.gov/pub/ASP%20Field%20Programs/2007CHAPS/).

EXPERIMENTAL APPROACH. CHAPS utilized a sampling strategy closely linking the DOE G-1, the National Aeronautics and Space Administration (NASA) B200 aircraft and primary and secondary surface sites. The G-1 made in situ measurements of particle concentrations, composition, particle and cloud droplet size distributions, optical properties, and cloud nucleating properties below, within, and above clouds downwind of Oklahoma City, while

the instrumentation on the B200 provided remotely observed profiles of aerosol extinction, backscatter, and depolarization over the same air space as that sampled by the G-1. Observations of boundary layer aerosols and meteorological conditions were made at the primary surface site just north of Oklahoma City and sky cover was measured at a nearby secondary surface site. Both surface sites were under the airspace in which observations were made by the two aircraft.

The in situ aircraft sampling strategy consisted of crosswind legs made below, within, and above fields of fair-weather clouds (FWCs). The lengths of these transects were designed to provide sufficient statistics for testing the fidelity of parameterizations used in large-scale models describing aerosol transport over distances typical of GCM grid cells (e.g., Berg and Stull 2002). By centering the campaign in the region close to Oklahoma City, the G-1 was able to make transects that passed through the urban plume. By extending the transects on either side of the Oklahoma City plume or by flying upwind of the city, in situ sampling was made in air that was characteristic of the regional-scale pollutant loading. Flight plans for the G-1 and B200 flights were coordinated so that the G-1 transects were within the aerosol backscatter, extinction, and depolarization "curtains" simultaneously measured by the high spectral resolution lidar (HSRL) on the B200 flying over the G-1.

G-1 instrumentation. Sampling of both activated and nonactivated particles was carried out during CHAPS through the use of two aerosol-sampling inlets on the G-1. Clear-air sampling was done through an isokinetic inlet (Brechtel Manufacturing, Hayward, CA; www.brechtel.com/Aerosol/Products/inlets.html), which uses a two-stage diffuser assembly to decelerate the airflow. No attempt was made to separate the cloud droplets from the air stream coming into this inlet when the G-1 was in clouds. Periods in which cloud drops entered the isokinetic inlet could be identified from the time series measured by the condensation particle counter (CPC), which shows sudden and very high particle number concentrations due to cloud droplets striking the inside of the inlet during passage through clouds.

A CVI inlet based on the design of Noone et al. (1993) was used for a second sampling line. This inlet uses a counterflowing air stream to selectively remove nonactivated particles from the sampling flow. Small particles and droplets (smaller than approximately 10 μm) are pushed out with the counterflow, while larger particles, including cloud droplets, pass through. The cloud droplets are then dried in a heated tube, leaving the aerosol kernel for analysis downstream. The water vapor from the evaporated drops was measured using a Maycomm tunable diode laser (TDL) hygrometer. The CVI inlet used during CHAPS was the same unit deployed by Hayden et al. (2008), who reported high levels of organics during ICARTT 2004. They attributed these high levels to the siloxane sealant used on the tip of the CVI. Aware of this problem, extensive cleaning and testing was conducted before CHAPS at the NOAA/Earth System Research Laboratory to ensure that the results collected during CHAPS would be free of this contamination.

The sampling streams from both inlets fed into essentially identical instrument systems for measuring the particle optical properties (Table 1), and each stream was sampled at reduced relative humidity (less than 40%). Aerosol absorption was measured using both a Radiance Research particle soot absorption photometer (PSAP) and a Droplet Measurement Technologies (DMT) photo-acoustic soot spectrometer.

The AMS was able to sample from either inlet stream depending on the position of a manually actuated value (flying with two AMS instruments was considered, but weight and space limitations precluded this option). This two-stream sampling necessitated making back-to-back flight legs in the cloud layer, one with the AMS sampling through isokinetic inlet followed by a return leg with the AMS sampling through the CVI inlet. Contamination from aircraft exhaust was considered, but given that the aircraft takes 3 min or more to turn and return to straight-and-level flight, there should be ample time for the exhaust to be transported away from the flight track that was oriented approximately perpendicular to the mean wind direction.

Additional instruments that sampled solely from the isokinetic inlet are described in Table 1; they include a DMT cloud condensation nuclei counter, a fast integrated mobility spectrometer (FIMS; Kulkarni and Wang 2006; Olfert et al. 2008), and a Scanning Mobility Particle Sizer (SMPS). These latter two aerosol-sizing instruments measured the size spectra of aerosol particles with diameters between 16 and 444 nm.

A proton transfer reaction mass spectrometer (PTR-MS) provided continuous measurements of many gas-phase organic species via a third inlet dedicated to gas-phase sampling that also included CO, SO_2, and O_3. While the relation of organic species and aerosols is part of the study, the gas phase

Table 1. Instruments deployed on the G-1 aircraft during CHAPS.		
Sampling stream	**Variable method**	**Instrument name**
Isokinetic and CVI	Aerosol absorption	Radiance Research Particle Soot Absorption Photometer (PSAP) and DMT and University Nevada–Reno photo-acoustic soot spectrometers
	Aerosol scattering	TSI 3563 three-wavelength integrating nephelometer
	Aerosol number	TSI 3010 condensation particle counter
	Aerosol composition	Aerodyne aerosol mass spectrometer
	Aerosol collection	Time-resolved aerosol collector (TRAC)
Isokinetic	Aerosol size distribution	Scanning Mobility Particle Sizer (SMPS) and Fast Integrated Mobility Spectrometer (FIMS)
	Cloud condensation nuclei	DMT dual-column cloud condensation nuclei counter
Chemistry	CO concentration	Vacuum UV fluorimeter
	O_3 concentration	2B Ozone analyzer
	SO_2 concentration	TEI 43S
	VOC concentration	Proton Transfer Reaction Mass Spectrometer (PTR-MS)
Aerosol, clouds, and precipitation	Size distributions of aerosols, cloud droplets, and precipitation	DMT Cloud, Aerosol, and Precipitation Spectrometer (CAPS), consisting of the Cloud Aerosol Spectrometer (CAS) and Cloud Imaging Probe (CIP)
	Aerosol size distribution	DMT Passive Cavity Aerosol Spectrometer Probe (PCASP-100X)
	Liquid water concentration	Gerber PVM-100A probe; also Maycomm TDL hygrometer on CVI
Meteorological variables	Turbulent winds	Gust probe
	Water vapor	Maycomm TDL, General Eastern 1011B chilled mirror
	Temperature	Platinum resistance thermometer
	Upwelling and downwelling UV radiation	Eppley radiometer

measurements are also being used to define when the G-1 was within the Oklahoma City plume.

Separate from the inlet-sampling instruments noted above were a number of instruments mounted on external pylons of the G-1, including a DMT Passive Cavity Aerosol Spectrometer Probe (PCASP-100X) to measure the particle number density for particles between 0.1- and 3-μm diameter and a DMT Cloud, Aerosol, and Precipitation Spectrometer (CAPS) to measure the distribution of cloud droplets with diameters ranging from 0.5 to 50 μm and precipitation particles between 25 and 1550 μm in diameter. A Gerber PVM-100A probe was used to measure the ambient liquid water content, and a second Maycomm TDL hygrometer was used to measure the water vapor content of the ambient air (the first TDL being associated with the CVI). The G-1 was also equipped with instruments to measure a number of meteorological parameters, including three-dimensional turbulent winds, ambient temperature, water vapor, pressure, and upwelling and downwelling UV radiation.

Prior to the campaign, there was concern that the G-1 would be in clouds for only short periods due to the airspeed (approximately 100 m s^{-1}) of the aircraft. This was an issue because the response time of many of the instruments deployed on the G-1 was 1 s or more and relatively small clouds were expected. This issue was highlighted by an earlier study by Berg and Kassianov (2008), who compiled a climatology of shallow clouds at the Atmospheric Radiation Measurement (ARM) Climate Research Facility (ACRF) Central Facility for the summers of 2000 through 2004. They found that the distribution of cloud chord lengths—defined by Berg and Kassianov (2008) as the cross-sectional length of a cloud that passes directly overhead—followed an exponential distribution and that the average cloud chord length was approximately 1 km. A similar analysis was conducted using data collected by the

G-1 and concluded that the mean cloud chord length sampled during CHAPS was 0.8 km, which is slightly less than expected from the climatology. The distribution, however, was still well described by an exponential distribution (not shown). Two strategies are being used to address the sampling issue during analysis of the CHAPS data. First, statistics are only computed for periods in which the cloud chord length was greater than approximately 500 m. Second, a digital inversion method (Shaw et al. 1998) has been applied to nephelometer data collected with the CVI and isokinetic inlets to deal with the instrument's large sample volume smearing the signal. This method reconstructs the signal assuming that the signal from the nephelometer behaves as a first-order differential equation (e.g., Bergin et al. 1997).

NASA King Air instrumentation. The NASA Langley Research Center's King Air B200 was equipped with the NASA Langley HSRL. The HSRL technique takes advantage of the spectral distribution of the lidar return signal to discriminate aerosol and molecular signals and thereby retrieve aerosol extinction and backscatter independently at a wavelength of 532 nm. This instrument also functions as a standard backscatter lidar at a wavelength of 1064 nm, enabling the calculation of the backscatter color ratio at these wavelengths. In addition, the lidar is polarization sensitive at both wavelengths (i.e., it measures the degree to which the backscattered light is depolarized from the linear polarized state of the transmitted pulses), enabling discrimination between spherical and nonspherical particles. The instrument parameters for the NASA Langley airborne HSRL instrument are shown in Table 2; Hair et al. (2006, 2008) provide a much more complete description of this system and how it is used to measure profiles of aerosol backscattering, extinction, and depolarization.

CHAPS surface site. Two CHAPS surface sites were deployed as part of the campaign in order to provide a baseline comparison for the aircraft data; these ground-based observations were continuous and closely paralleled many of the aerosol optical properties measured with the G-1. Both of the ground sites were set up specifically for CHAPS and were located north of Oklahoma City to increase the chance sampling would occur within the Oklahoma City plume during conditions with southerly winds. The primary site was located north of Edmond, Oklahoma (35.73°N, −97.48°W), while the secondary site was located at the University of Central Oklahoma in Edmond (35.67°N, −97.47°W). The instruments deployed at the sites are listed in Table 3. Much of the instrumentation at the ground sites was similar to those deployed at the ACRF Southern Great Plains (SGP) Central Facility as described by Sheridan et al. (2001), including a micropulse lidar (MPL). This strategy was designed to facilitate a comparison of observations near Oklahoma City, with the background values more characteristic of the SGP site. Unfortunately, large amounts of precipitation during CHAPS made it difficult to adequately dry the airstream sent to the nephelometer and PSAP, which complicates the analysis of scattering and absorption

Table 2. System parameters for the airborne HSRL.

Transmitter	
Repetition rate	200 Hz
532-nm energy	2.5 mJ
1064-nm energy	1 mJ
Optical receiver	
Telescope	0.4-m diameter
532 etalon FWHM	40 pm
1064 IF FWHM	1 nm
Detection electronics	
532 nm	Photomultiplier tube (PMT) with analog detection
1064 nm	Avalanche photo diode (APD) with analog detection

Table 3. Instruments deployed at the primary and secondary CHAPS surface sites.

Variable measured	Instrument name
Aerosol absorption	Radiance research PSAP
Aerosol scattering	TSI 3563 three-wavelength integrating nephelometer
Particle number concentrations	TSI 3010 condensation particle counter
Temperature/humidity	Vaisala radiosonde system
Wind profiles	915-MHz wind profiler
Aerosol backscatter profile	Micropulse lidar

measurements made at the CHAPS surface site. A total sky imager was deployed a few kilometers from the primary surface site. This instrument provided time-dependent hemispheric views of the sky, as well as estimates of cloud fraction and cloud aspect ratio. The imager was deployed at the secondary site to allow for high-speed Internet access that was needed for data quality control purposes.

The MPL at the CHAPS surface site was modified to include a pointing and scanning capability. This allowed the MPL to observe spatial differences in mixed layer development (by scanning in predetermined sequences) and provided a means by which observations of individual clouds and their immediate surroundings could be made. Using a real-time video camera mounted on the MPL's telescope allowed for measurements to by made around cloud edges, resulting in the identification of several instances associated with well-defined inflow of aerosols into clouds. The 915-MHz radar wind profiler (RWP) was configured to provide 30-min-averaged wind profiles calculated from 30-s-averaged spectra from beams pointed sequentially north, west, south, and east, tilted 24° from vertical followed by a vertically pointed sample. Although not ideally configured for obtaining estimates of vertical velocity, it was possible to combine data from the two instruments, which are described in the "Preliminary findings" section.

Flight patterns. Three flight patterns were used during CHAPS (Fig. 1). The first pattern consisted of straight-and-level flight legs flown at three altitudes, including a low-level flight approximately 100–600 m below cloud base, two back-to-back legs through the cloud fields, and another leg flown at an altitude selected to be above the majority of clouds—although, as would be expected from the characteristically wide range of cloud-top heights associated with cumuli, there were a number of instances in which the G-1 intersected clouds during this highest leg.

Frequently, one set of stacked legs (below cloud/in cloud with AMS sampling from the CVI/in cloud with AMS sampling from the isokinetic inlet/above cloud) was flown upwind of Oklahoma City, and two sets of legs were flown downwind of the city. This pattern let us sample the regional air upwind of the city as well as the more polluted conditions downwind. The second pattern was a "half-hexagon" flown entirely downwind of the city (see Fig. 1 for the basis of this name). Regional air for this pattern was encountered as the hexagon wrapped around Oklahoma City, with the ends of these flight legs outside of the plume, as indicated by the CO concentration. These half-hexagonal patterns also had one leg below cloud base, two legs through the cumuli, and one leg above cloud top. This pattern was designed to increase the probability that the aircraft would intersect the Oklahoma City plume.

The third flight pattern was designed as part of a related experiment to make concurrent observations from the G-1 and King Air, in conjunction with observations made from aircraft in the field for the ARM Clouds and Land Surface Interaction Campaign (CLASIC) study. Both CHAPS and CLASIC were designed to investigate shallow cumuli. Whereas CHAPS was focused on how clouds change the aerosol properties, the CLASIC was designed to investigate the relationship between clouds and the processes at the surface. Five additional aircraft participated in the CLASIC, including the NASA ER-2, Center for Interdisciplinary Remotely Piloted Aircraft Studies (CIRPAS) Twin Otter, Twin-Otter International,

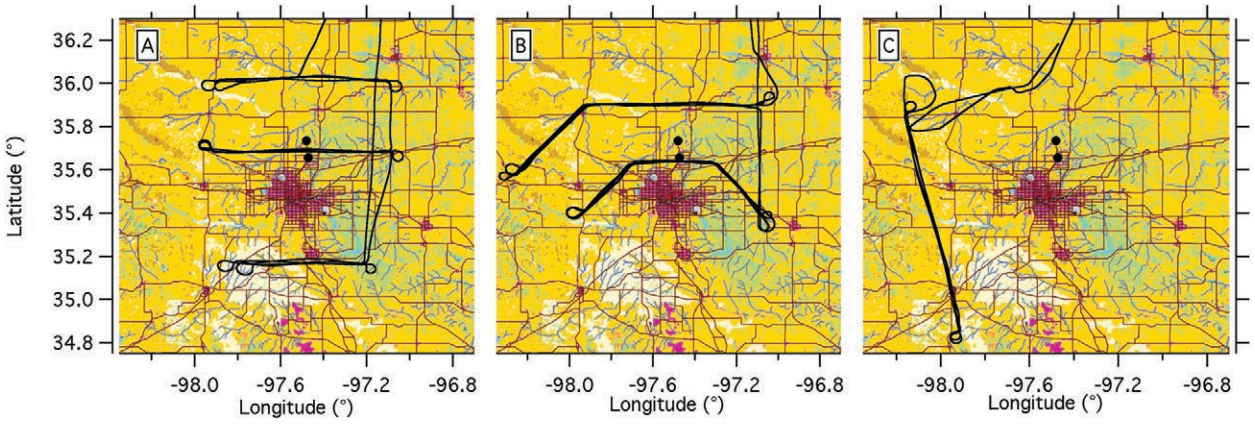

Fig. 1. Representative flight patterns flown by the G-1 during CHAPS; (a) 20 Jun, (b) 25 Jun, and (c) 19 Jun. Circles indicate the location of the CHAPS surface sites. Colors indicate land use, with magenta indicating Oklahoma City and other colors representing various surface types (e.g., croplands, pastures, or forests).

Duke Bell Helicopter, and the ARM Cessna 206. Details of the payloads carried by these aircraft can be found in Miller et al. (2007). Scientists associated with both CHAPS and CLASIC have a common interest in understanding observations made from the NASA Satellite A-Train and pooled their airborne resources in a coordinated pattern designed to relate in situ measurements with observations made by the A-Train. One flight plan involved making simultaneous stacked measurements of aerosol extinction from each aircraft platform concurrent with the A-Train satellite overpass. This mission is discussed more fully in the "Preliminary results" section.

We should note that many of the measurements made during CLASIC augment the data collected during CHAPS and vice versa. The NASA ER-2 overflights included passes over the domain sampled by both the G-1 and the King Air. The Moderate Resolution Imaging Spectoradiometer (MODIS) Airborne Simulator was deployed on the ER-2, providing a high-resolution view of large areas of shallow clouds.

WEATHER CONDITIONS. June 2007 was the wettest June on record for much of Oklahoma. Approximately 33 cm of rain fell on central Oklahoma, which is nearly 20 cm more than average (Oklahoma Climatological Survey; see http://climate.ok.gov). A persistent region of high pressure was located over the southeastern United States for most of June. The pressure gradient associated with this pattern led to generally southeasterly winds near the surface and significant low-level moisture advection from over the Gulf of Mexico. In addition to this low-level pattern, a number of slow-moving upper-level lows contributed to the large amount of rainfall. The majority of the CHAPS flights were conducted during two periods, 6–12 and 19–24 June, during which there was a weak ridge in the 500-mb pattern that led to some drying and an increase in the frequency of FWCs.

PRELIMINARY RESULTS. *Oklahoma City plume.* Basic to our analysis is the capability to distinguish between regional air and air from within the Oklahoma City plume. Evidence of the latter was found on nearly every flight. An example showing observations of CO (commonly associated with urban emissions) collected during a subcloud leg on 23 June is shown in Fig. 2 (the missing data near longitude −97.7° was due to a turn that the G-1 made in the middle of the leg). During this leg, CO values of approximately 110 ppbv were observed during the first part of a transect made below cloud base, downwind of Oklahoma City, with an increase to 170 ppbv highlighted by the shading in Fig. 2. Concurrent with this increase in CO were increases in number concentration of small particles measured by the FIMS and particle absorption, as well as a decrease in the single scattering albedo (SSA) computed using the scattering at a wavelength of 550 nm and absorption at a wavelength of 532 nm (the difference between the absorption at 550 and 532 nm is small, so no wavelength adjustment was applied in this analysis). The observed decrease in SSA is assumed to represent relatively fresh, "unprocessed" atmospheric aerosols emanating from Oklahoma City. Support for this assumption comes from an examination of the aerosol size distribution measured by the SMPS, FIMS, and PCASP, which indicate an increase of nearly an order of magnitude in the number of particles with diameter less than 0.03 μm in the Oklahoma City plume (Fig. 3) compared to conditions in regional air. There were negligible differences in the number of particles with diameters greater than 0.05 μm. Individually, small particles scatter less light and fresh particles are

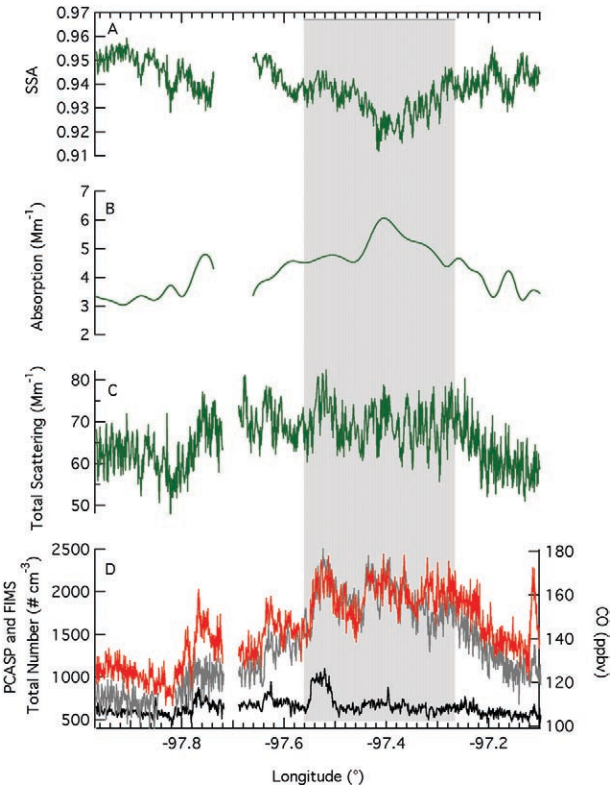

Fig. 2. Time series of (a) single scattering albedo, (b) absorption at 532 nm, (c) total scattering at 550 nm, and (d) PCASP total number concentration (black line), FIMS total number concentration (red line), and CO concentration (gray line) measured during a subcloud leg (~400 m above ground) on 23 Jun 2007 between 1638 and 1657 UTC. Shading indicates periods associated with the Oklahoma City plume.

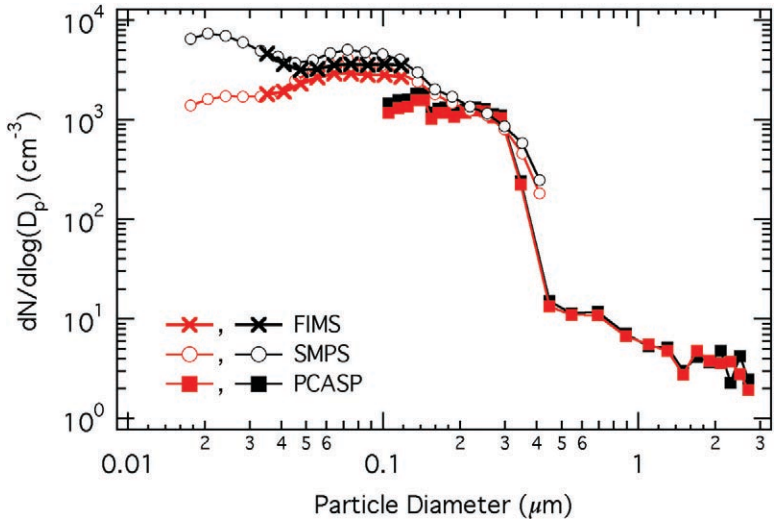

Fig. 3. Below-cloud aerosol size distributions inside (black) and outside (red) the Oklahoma City plume measured in a subcloud leg on 23 Jun 2007. Symbols indicate which instrument—FIMS (X), SMPS (circles), or PCASP (squares)—was used to measure the size distribution.

generally more light absorbing than aged particles. We believe this leads to the observed increase in aerosol absorption with little change in the observed scattering, resulting in a reduced SSA. Some care must also be exercised when comparing the results from the FIMS and SMPS to the PCASP because of different sampling conditions. The FIMS and SMPS were located inside the G-1 and measure the dry aerosol size distribution, whereas the PCASP measures the aerosol size distributions at conditions closer to ambient. However, the PCASP was operated with de-icing heaters turned on, causing some drying of the particles, so the sampling conditions of the PCASP were not truly ambient either.

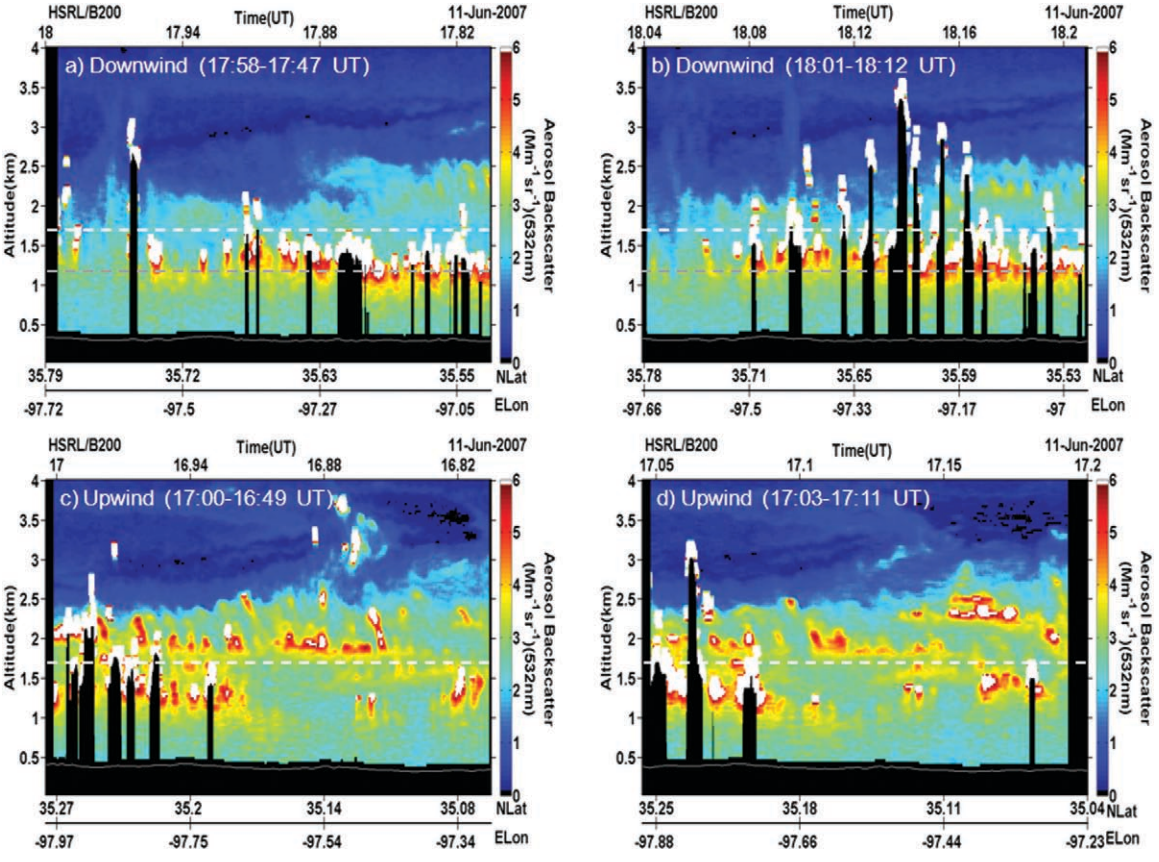

Fig. 4. Aerosol backscatter profiles derived from HSRL measurements on 11 Jun measured (a), (b) downwind and (c), (d) upwind of Oklahoma City (OKC). West (east) is on the left (right) side of these images. Time increases to the right for (b) and (d) and to the left for (a) and (c). The altitude of the G-1 legs through the cloud layer is shown by the dashed white lines, and the altitude of the G-1 during the downwind subcloud leg is shown by the dashed gray line.

As was the case on 23 June, the small size of the particles on 11 June made it difficult to identify the Oklahoma City plume in the HSRL cross sections (Fig. 4) and to differentiate between the upwind and downwind legs based on aerosol backscatter alone. Although an increase in backscatter with height was observed by the HSRL, this behavior was probably associated with the hygroscopic growth of the aerosols. Figures 4a,b also show a gradient of aerosol backscatter below the clouds. This gradient could be the result of changes in the boundary layer humidity (note that there are many more clouds on the eastern half of the domain) or changes in the amount of aerosols. Figure 5 shows the dry aerosol scattering measured by the G-1 during the below cloud leg corresponding to Fig. 4a. There is a decrease in the dry scattering and the CO concentration near the western edge of the flight leg (as indicated by the arrow). The G-1 also measured a gradient of relative humidity from west to east. There are also a number of oscillations that appear in total scattering, relative humidity, and CO. This leg was flown near cloud base, close to the boundary layer top, and it is likely that these oscillations are due to relatively clean air being entrained into the boundary layer.

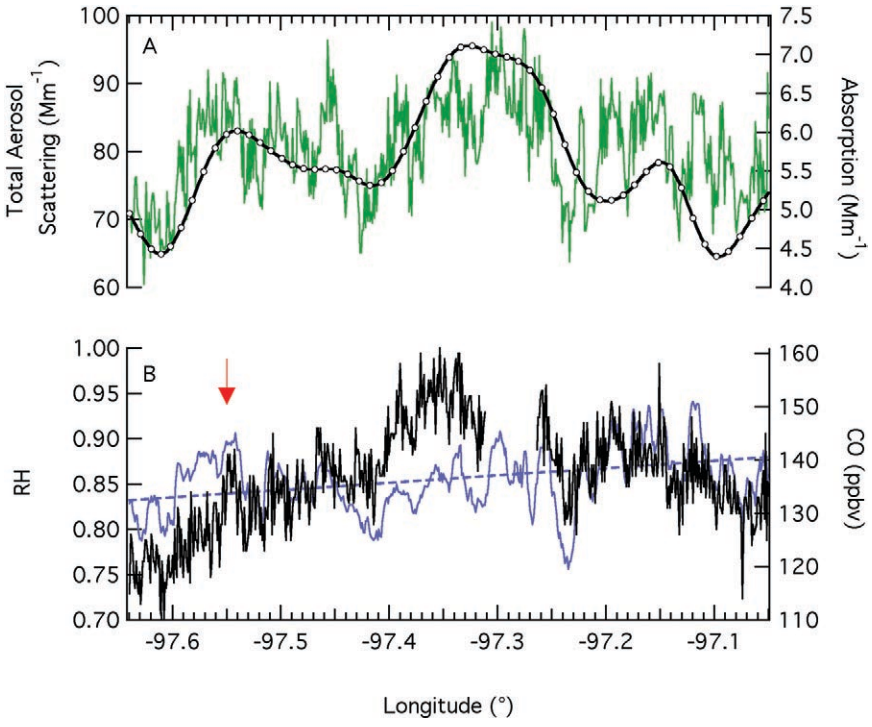

Fig. 5. Plot, as function of longitude, of (a) total aerosol scattering (green line, left axis) at 550 nm and smoothed aerosol absorption (black line, right axis) at 532 nm and (b) relative humidity (blue, left axis) and CO (black, right axis) measured by the G-1 for the subcloud leg flown on 11 Jun. The arrow indicates a decrease in the observed scattering and CO, and the dashed line is a least-squares best fit to the relative humidity; see the text for details.

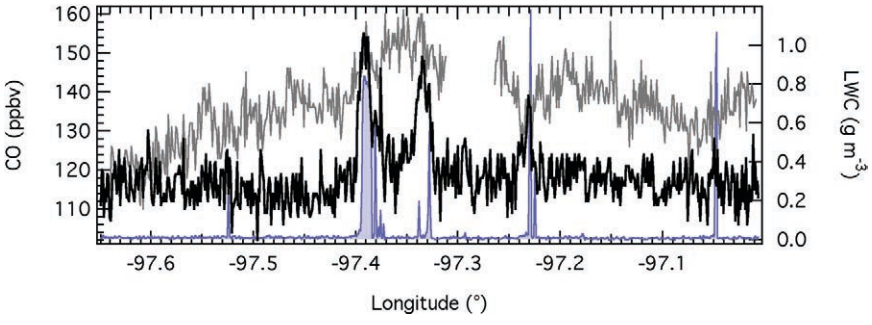

Fig. 6. Below-cloud (gray) and cloud layer (black) CO and liquid water content (LWC; blue) measured by the Gerber probe as a function of longitude on 11 Jun.

Evidence of cloud processing. A goal of CHAPS was to identify aerosols that had undergone processing by clouds. Clear evidence of cloud samples within the urban plume was encountered during the flight of 11 June. On this day the cloud fraction measured by the G-1 was relatively small, approximately 5% based on the fraction of time that the cloud-layer legs were inside clouds. The FWC that the G-1 encountered downwind of Oklahoma City showed well-defined elevated levels of CO (Fig. 6) with concentrations characteristic of the values measured below the clouds, indicating that the clouds are acting as conduits, transporting relatively dirty air up from the boundary layer to cloud top.

The efficiency with which particles are activated to form cloud droplets is a parameter of interest to scientists studying the interactions of aerosols and clouds.

One way to evaluate the fraction of particles activated into droplets is to compare the ratio of the number concentration of cloud drops to the total number of accumulation mode particles (defined to be particles with diameter between 0.5 and 2 μm; Glickman 2000) measured below the clouds. This ratio is commonly called the activation fraction. Given that many CCN are smaller than 0.5 μm, the activation fraction can be greater than 1 because some of the smaller, and therefore uncounted, particles will also be activated. The methodology used here is the same as the droplet activation fraction defined by Raga and Jonas (1993) and applied by Lu et al. (2008). Following Lu et al. (2008), the total number of particles measured by the PCASP, which measures the aerosol size distribution for particle diameters between 0.1 and 3 μm, was used to represent the total number of particles in the accumulation mode. The number of cloud droplets was computed by integrating the size distribution measured by the CAS. To provide consistency with the range of cloud drop sizes that have been used previously in the literature (e.g., Raga and Jonas 1993; Lu et al. 2008), and to eliminate large haze drops, only particles measured by the Cloud and Aerosol Spectrometer (CAS) that were greater than 5 μm and less then 40 μm in diameter were included. Because of the time required for each transect (approximately 15 min) and the relatively constant value of the number concentration observed in the below-cloud layer (Fig. 7), the average particle number concentration measured by the PCASP was assumed to be representative of the entire flight leg. Figure 7 shows the activation fraction for one flight leg through clouds on 11 June. The value ranges from 1.4 to 0.2 and the leg average is 0.71, which is consistent with the values reported by Raga and Jonas (1993) and Lu et al. (2008).

The AMS provided a measure of the nonrefractory composition of the aerosols that passed through the isokinetic or CVI inlets. The AMS, however, does not detect refractory materials, such as black carbon, sodium chloride, and mineral dust. Results from the paired upwind and downwind transects made on 11 June are presented in Fig. 8. On this day, the total aerosol mass decreases with height (not shown). Sulfate and organics dominate the mix of the nonrefractory part of the aerosols both upwind and downwind of Oklahoma City at all altitudes studied. However, the fractional amount of sulfate relative to the other components is smaller and the fractional amount of organics is larger downwind of Oklahoma City, indicating that a large fraction of the aerosol mass produced in the vicinity of Oklahoma City is organic. There is also an increase in the mass fraction of nitrate within the cloud drops sampled by the CVI. The increase in nitrate mass is likely due to the uptake of gas phase nitric acid, which in turn is created from oxidation of NO_x generated from combustion, into the cloud drops and the subsequent neutralization of the nitrate by ammonium (Seinfeld 1986). The ratio of the ammonium to sulfate measured by the AMS provides some insight into the amount of ammonium and its potential to neutralize both the sulfate and nitrate. A value of 2 indicates that the aerosols are of near-neutral pH (e.g., Seinfeld 1986). The ratio was found

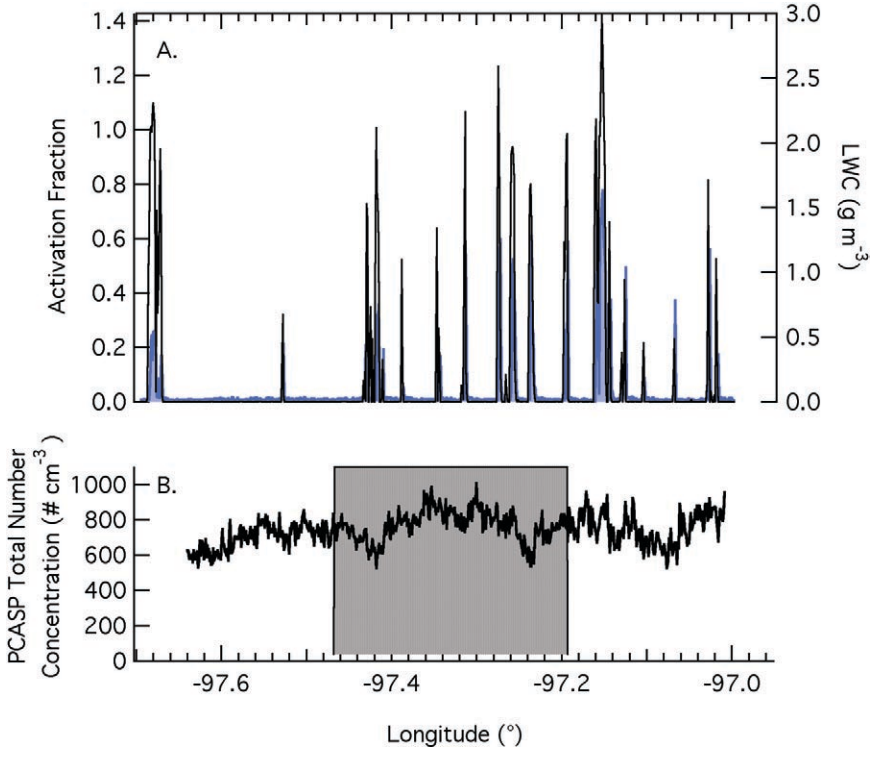

FIG. 7. (a) Activation fraction (black line, left axis) and LWC measured by the Gerber probe (blue, right axis) and (b) PCASP total number concentration measured in the subcloud layer as a function of longitude on 11 Jun 2007. Shading shows the approximate extent of the subcloud plume.

to be less than 2 below clouds and slightly larger than 2 within the clouds, indicating that there was sufficient ammonium to produce the observed nitrate in the aerosol kernels.

A-Train intercomparison flights. There were a number of opportunities during CHAPS for intercomparison flights with the NASA A-Train satellites. The results from one such comparison are shown in Fig. 9. These observations were made on 19 June using the aircraft stacked pattern described earlier and provide a comparison of measurements made from the Cloud–Aerosol Lidar with Orthogonal Polarization (CALIOP) system on the Cloud–Aerosol Lidar and Infrared Pathfinder Satellite (CALIPSO). The flight altitudes of the G-1, CIRPAS Twin Otter, and ARM Cessna 206 during the CALIPSO overflight are shown by arrows in Fig. 9, and the attenuated backscatter profiles from the CALIPSO lidar are shown along with the corresponding profiles from the airborne HSRL.

During this flight over central Oklahoma and Kansas, considerable low-level broken clouds were observed and also detected by the HSRL and CALIPSO lidar measurements. In this example, the CALIPSO lidar vertical feature finder has identified broken clouds between 1 and 3 km and has identified an elevated aerosol layer near 4 km over Kansas. The CALIPSO profiles have 5-km horizontal resolution in contrast to the 1-km resolution of the HSRL profiles. Consequently, the higher HSRL resolution permits more measurements between clouds, as shown by the yellow colors between clouds in Fig. 9b. Figure 9e also shows good agreement between the attenuated backscatter profiles averaged over this flight track from both lidar systems. We expect that data collected during the CHAPS and CLASIC missions will be useful for evaluating the aerosol and cloud measurements acquired by the CALIPSO lidar and other A-Train sensors.

Surface site. While data from the airborne instruments are very useful for evaluating in-cloud, out-of-cloud, below-cloud, and above-cloud differences, continuous observations from the CHAPS surface sites provide complementary information about the clouds and aerosols. One particularly useful measurement to come from the surface site is the estimate of the inflow into shallow cumuli made utilizing the MPL data. One such case was observed on 22 June. In this case the MPL was held stationary for more than 3 h (1845–2210 UTC) and pointed toward the southwest with an elevation angle of 30.7°. Near the surface,

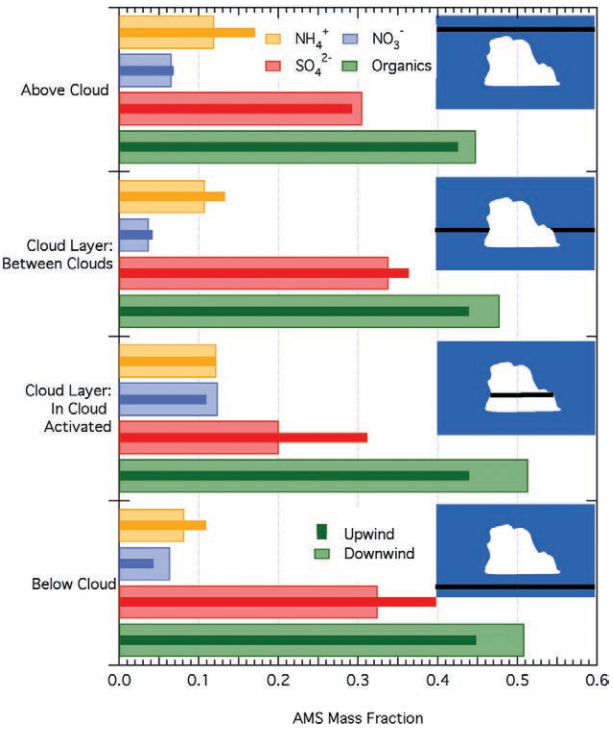

Fig. 8. (bottom) Mass fraction (μg of component species to total μg measured by the AMS) of organics (green), SO_4^{2-} (red), NO_3^- (blue), and NH_4^+ (yellow) observed on 11 Jun 2007 upwind (thick bars) and downwind (thin bars) of Oklahoma City below cloud. Activated aerosols in clouds and areas (middle) between clouds and (top) above cloud. Black lines on inset pictures illustrate source regions of data.

the winds were southerly at 7 m s^{-1} and backed with height to southwesterly at 10 m s^{-1} near 1.5 km above the surface. The geometry of the MPL and the wind direction resulted in clouds moving directly toward the MPL. The cloud-base height observed during this period rose slightly from 800 to 1,000 m. Cloud tops, estimated from the topmost points of contiguous returns as the clouds moved through the MPL beam, were near 1.5 km (which corresponded to the height of the maximum wind speed).

The MPL returns for the period between 1936 and 2000 UTC are shown in Fig. 10. These clouds are located at the top of boundary layer thermals that have a base well within the mixed layer, as shown by the streaks of enhanced aerosol backscatter below the clouds. The streaks themselves are likely due to particles that are growing within the thermal as the relative humidity increases with height as the air rises in the boundary layer. The apparent tilt of the inflow and thermals is associated with the angle of the MPL from horizontal into the wind. If it is assumed that the plumes are perfectly vertical, then the mean wind

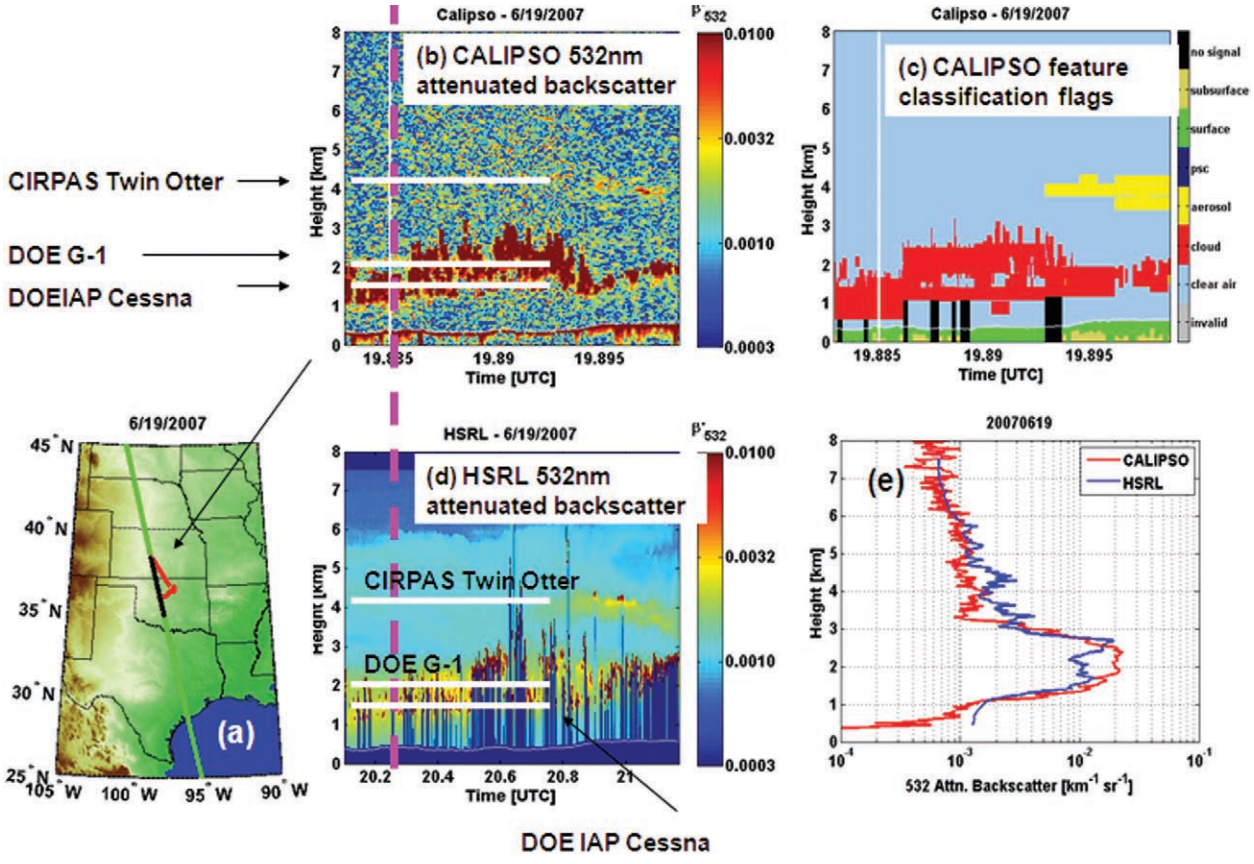

Fig. 9. Results from CALIPSO intercomparisons. Map showing CALIPSO ground track (green), B200 flight track (red), and track of joint HSRL/CALIPSO lidar comparisons (black); (b) CALIPSO lidar attenuated backscatter profiles (km sr)$^{-1}$ (532 nm). Each profile represents the running average of 15 0.33-km CALIPSO lidar profiles. The approximate altitudes of three other coordinated aircraft are also shown. The vertical purple line shows the exact coincidence time. (c) Atmospheric feature classification as determined by the CALIPSO vertical feature finder and (d) HSRL attenuated backscatter profiles (532 nm) with 1-km horizontal resolution. (e) Comparison of CALIPSO lidar and HSRL attenuated backscatter profiles (532 nm) averaged over the track of joint lidar operations.

speed can be calculated from the difference in time indicated by the intersection of the top and bottom of the plume. Using typical values of height and time difference gives a wind speed estimate of approximately 7 m s^{-1}, which agrees well with the wind speed observed by the radar wind profiler.

The instrument configuration at the main CHAPS surface site precluded simultaneous observations of the same cloud with the RWP and the MPL. However, individual estimates of vertical velocity (w) can be made from the RWP during this period. Each estimate is representative of only a 30-s time period, separated by 150 s; thus, it is possible, even likely, that a direct measure of w during a single cloud passage above the RWP did not occur. Furthermore, the intersection of any given cloud base with the profiler beam will seldom encompass a large portion of a given cloud. Several possible times for cloud inflow were chosen based solely on the maximum values of w. Figure 11 shows the vertical profiles of w and signal return for each of these times. All of the instances are associated with upward motion within the mixed layer, usually with maxima of 1.5–2 m s^{-1} at or below cloud base (as defined from Fig. 10). The profiles at 1854 and 1916 UTC have significant upward motion beginning as low as 200 m (the lowest range gate). Signal amplitudes at 1854 UTC display maxima just below cloud base and again at or above cloud top; this points to relatively large amounts of turbulence associated with inflow and entrainment regions.

CONCLUSIONS. The summer 2007 CHAPS campaign was designed to collect observations relevant to a number of issues related to aerosols and clouds, including differences in below-cloud aerosol optical and cloud nucleating properties downwind of Oklahoma City, the distribution of aerosol extinction in the vicinity of shallow clouds, and differences in aerosol op-

tical properties inside and outside of the Oklahoma City plume. Our review of these observations suggests that the resulting rich data are suitable for further in-depth analysis, including model studies related to the activation of aerosols as they are lifted up from the convective boundary layer into the clouds, the chemical uptake of gaseous nitric acid, the transport of aerosols moving with the boundary and layer thermals into the shallow clouds, and changes in the size distribution of aerosols upwind and downwind of Oklahoma City, as well as decreases in single scattering albedo and increases in aerosol absorption.

In addition to the primary research goals of CHAPS, there was a unique opportunity to conduct some G-1 and King Air flights for validation of the NASA satellite A-Train. A successful satellite intercomparison flight, conducted in coordination with CLASIC, was completed and selected results presented. During this flight good agreement between the CALIPSO lidar and the HSRL was shown.

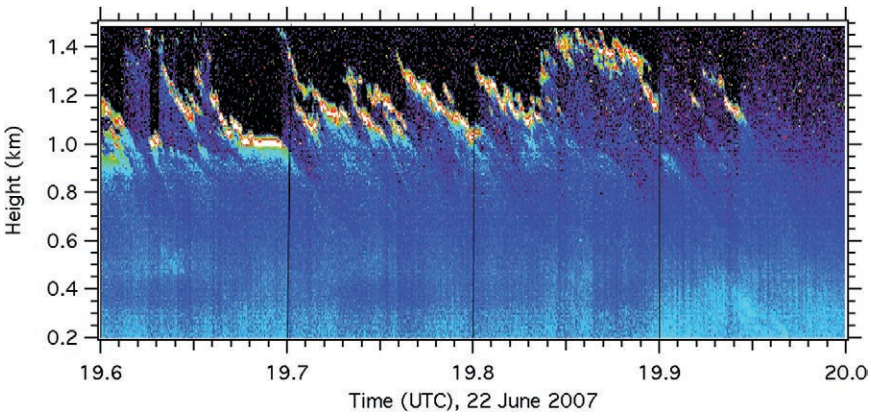

Fig. 10. Range-corrected MPL returns from within the mixed and cloud layer above the surface site on 22 Jun 2007 during the CHAPS field study. The MPL was tilted at an elevation angle of 30°. Data have been converted to height above the surface, thus returns from 1.5 km are about 2.6 km upwind.

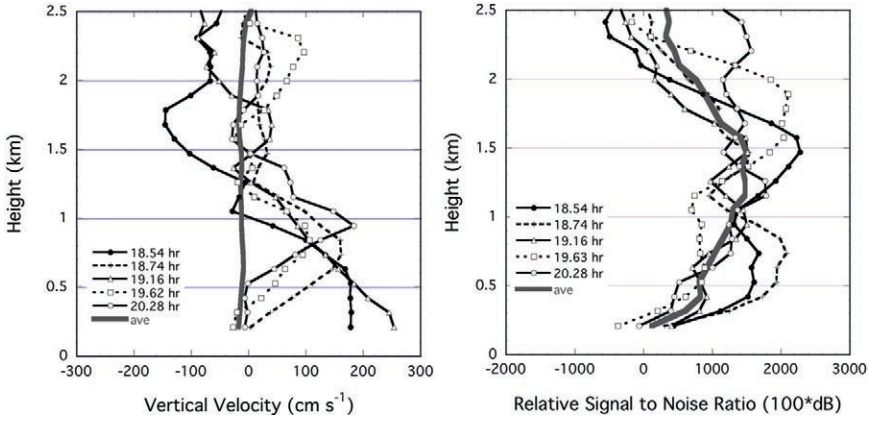

Fig. 11. Thirty-second profiles of (left) vertical velocity and (right) range-corrected signal amplitude derived from RWP data collected on 22 Jun. These periods (as defined in the legend) were selected because they were periods during which cloud inflow was likely to be captured.

ACKNOWLEDGMENTS. Much of the success of CHAPS can be attributed to the aircrews of the G-1, Mr. Robert Hannigan and Richard Hone and the NASA King Air (Mr. Mike Wusk, Rick Yasky, Les Kagey, Howard Lewis, Scott Sims, and Dale Bowser), and the close cooperation of the team leading CLASIC, including Drs. Mark Miller of Rutgers University, Peter Lamb of the University of Oklahoma, and Beat Schmid and James Mather of PNNL. A number of scientists, including Drs. Gunnar Senum of Brookhaven National Laboratory (BNL), Connor Flynn, Alexander Laskin, and Yury Desyaterik of PNNL, and John Jayne of Aerodyne, worked diligently to ensure that equipment was operating properly. Drs. Peter Daum and Lawrence Kleinman of BNL provided guidance during the deployment. Ms. Debbie Ronfeld of PNNL provided logistical support in the field. Mr. Chuck Greenwood and staff at Greenwood Aviation provided hanger and office space and ground support for the aircraft operations. We thank Dr. Pat Arnott from the University of Nevada–Reno for providing one of the photoacoustics on board the aircraft and Ian McCubbin from the Desert Research Institute of Reno, Nevada, for his contribution in operating the DMT photoacoustic instrument. Dr. Patric Sheridan (NOAA/ESRL) led efforts to calibrate the optical instruments used during both CHAPS and CLASIC. The primary CHAPS surface site was deployed on land owned by Mr. Bob Brentlinger by Drs. Mikhail Pekour and William Shaw of PNNL and Tim Martin of Argonne National Laboratory. Prof. Baha Jassemnejad of the University of Central Oklahoma was instrumental in making arrangements for the secondary surface site. Dr. Charles Long of PNNL assisted with the deployment of the Total

Sky Imager. We also thank the Department of Energy Atmospheric Science Program, which is part of the Office of Biological and Environmental Research, Climate and Environmental Sciences Division, as well as the NASA HQ Science Mission Directorate Radiation Sciences Program, and the NASA CALIPSO project for funding portions of this research. The Pacific Northwest National Laboratory is operated by Battelle Memorial Institute for the U.S. Department of Energy under Contract DE-AC05-76RL01830. We thank Dr. Nels Laulainen for numerous discussions related to this work. Comments from two anonymous reviewers also improved this manuscript.

REFERENCES

Alkezweeny, A. J., D. A. Burrows, and C. A. Grainger, 1993: Measurements of cloud-droplet-size distributions in polluted and unpolluted stratiform clouds. *J. Appl. Meteor.,* **32,** 105–115.

Berg, L. K., and R. B. Stull, 2002: Accuracy of point and line measures of boundary layer cloud amount. *J. App. Meteor.,* **41,** 640–650.

——, and E. I. Kassianov, 2008: Temporal variability of fair-weather cumulus statistics at the ACRF SGP site. *J. Climate,* **21,** 3344–3358.

Bergin, M. H., J. A. Ogren, S. E. Swartz, and L. M. McInnes, 1997: Evaporation of ammonium nitrate aerosol in a heated nephelometer: Implications for field measurements. *Environ. Sci. Tech.,* **31,** 2878–2883.

Fehsenfeld, F. C., and Coauthors, 2006: International Consortium for Atmospheric Research on Transport and Transformation (ICARTT): North America to Europe: Overview of the 2004 summer field study. *J. Geophys. Res.,* **111,** doi:10.1029/2006JD007829.

Forster, P. V., and Coauthors, 2007: Changes in atmospheric constituents and in radiative forcing. *Climate Change 2007: The Physical Science Basis,* S. Solomon et al., Eds., Cambridge University Press, 153–171.

Ghan, S. J., and S. E. Schwartz, 2007: Aerosol properties and processes a path from field and laboratory measurements to global climate models. *Bull. Amer. Meteor. Soc.,* **88,** 1059–1083.

Glickman, T., Ed., 2000: *Glossary of Meteorology.* American Meteorological Society, 850 pp.

Hair, J., C. Hostetler, R. Ferrare, A. Cook, and D. Harper, 2006: The NASA Langley high spectral resolution lidar for measurements of aerosols and clouds. *Proc. 23rd Int. Laser Radar Conf.* 411–414.

——, and Coauthors, 2008: Airborne high spectral resolution lidar for profiling aerosol optical properties. *Appl. Opt.,* **36,** 6734–6752.

Hayden, K., and Coauthors, 2008: Cloud processing of nitrate. *J. Geophys. Res.,* **113,** D18201, doi:10.1029/2007JD009732.

Huebert, B. J., T. Bates, P. B. Russell, G. Shi, Y. J. Kim, K. Kawamura, G. Carmichael, and T. Nakajima, 2003: An overview of ACE-Asia: Strategies for quantifying the relationship between Asian aerosols and their climatic impacts. *J. Geophys. Res.,* **108,** 8633, doi:10.1029/2003JD003550.

Jayne, J. T., D. C. Leard, X. Zhang, P. Davidovits, K. A. Smith, C. E. Kolb, and D. R. Worsnop, 2000: Development of an aerosol mass spectrometer for size and composition analysis of submicron particles. *Aerosol Sci. Technol.,* **33,** 49–70.

Jirak, I. L., and W. R. Cotton, 2006: Effect of air pollution on precipitation along the Front Range of the Rocky Mountains. *J. Appl. Meteor. Climatol.,* **45,** 236–245.

Kulkarni, P., and J. Wang, 2006: New fast integrated mobility spectrometer for real-time measurement of aerosol size distribution. I: Concept and theory. *J. Aerosol Sci.,* **37,** 1303–1325.

Lu, M.-L., G. Feingold, H. H. Jonsson, P. Y. Chuang, H. Gates, R. C. Flagan, and J. H. Seinfeld, 2008: Aerosol–cloud relationships in continental shallow cumulus. *J. Geophys. Res.,* **113,** D15201, doi:10.1029/2007JD009354.

Miller, M. A., and Coauthors, 2007: SGP Cloud and Land Surface Interaction Campaigns (CLASIC). U.S. Department of Energy, DOE/SC-ARM-0703, 14 pp.

Molina, L. T., S. Madronich, J. S. Gaffny, and H. B. Singh, 2008: Overview of the MILAGRO/INTEX-B campaign. *IGAC Newsletter,* No. 38, International Global Atmospheric Chemistry Project, Taipei, Taiwan, 2–15.

Noone, K. B., K. J. Noone, and J. A. Ogren, 1993: In-situ observations of cloud microphysical properties using the counterflow virtual impactor. *J. Atmos. Oceanic Technol.,* **10,** 294–303.

Olfert, J. S., P. Kulkarni, and J. Wang, 2008: Measuring aerosol size distributions with the fast integrated mobility spectrometer. *J. Aerosol Sci.,* **39,** 940–956, 10.1016/j.jaerosci.2008.06.005.

Raes, F., T. Bates, F. McGovern, and M. C. Liedekerke, 2000: The Second Aerosol Characterization Experiment (ACE 2); General overview and main results. *Tellus,* **52B,** 111–125.

Raga, G. B., and P. R. Jonas, 1993: On the link between cloud-top radiative properties and sub-cloud aerosol concentrations. *Quart. J. Roy. Meteor. Soc.,* **199,** 1419–1425.

Seinfeld, J. H., 1986: *Atmospheric Chemistry and Physics of Air Pollution.* Wiley, 768 pp.

Shaw, W. J., C. W. Spicer, and D. V. Kenny, 1998: Eddy

correlation fluxes of trace gases using a tandem mass spectrometer. *Atmos. Environ.,* **32,** 2887–2898.

Sheridan, P. J., D. J. Delene, and J. A. Ogren, 2001: Four years of continuous surface aerosol measurements from the Department of Energy's Atmospheric Radiation Measurement Program Southern Great Plains Cloud and Radiation Testbed site. *J. Geophys. Res.,* **106,** 20 735–20 747.

Sorooshian, A., N. L. Ng, A. W. H. Chan, G. Feingold, R. C. Flagan, and J. H. Seinfeld, 2007: Particle organic acids and overall water-soluble aerosol composition measurements from the 2006 Gulf of Mexico Atmospheric Composition and Climate Study (GoMACCS). *J. Geophys. Res.,* **112,** D13201, doi:10.1029/2007JD008537.

Van Den Heever, S. C., and W. R. Cotton, 2007: Urban aerosol impacts on downwind convective storms. *J. Appl. Meteor. Climatol.,* **46,** 828–850.